Research Article

Asmawi Nazrin, Salit Mohd Sapuan*, Mohamed Yusoff Mohd Zuhri, Intan Syafinaz Mohamed Amin Tawakkal, and Rushdan Ahmad Ilyas

Water barrier and mechanical properties of sugar palm crystalline nanocellulose reinforced thermoplastic sugar palm starch (TPS)/poly (lactic acid) (PLA) blend bionanocomposites

https://doi.org/10.1515/ntrev-2021-0033
received April 27, 2021; accepted May 16, 2021

Abstract: The disposal of non-biodegradable synthetic plastic wastes is linked with air, land, and marine pollutions. Incineration of plastic wastes released toxic substances into the air while recycled plastics end up accumulated in landfill and dumped into the ocean. In this study, novel sugar palm starch reinforced with sugar palm crystalline nanocellulose was blended with poly(lactic acid) (PLA) with various formulations to develop alternative materials potentially substituting conventional plastics. X-ray diffraction analysis demonstrated broad amorphous scattering background with minor diffraction peaks at 2θ of 19.4° and 22° associated with V_H-type and B-type crystal structure for all blend bionanocomposites samples. Higher solubility rates were observed for PLA20TPS80 (96.34%) and PLA40TPS60 (77.66%) associated with higher concentration of plasticizers providing extra space in the polymer chains to be penetrated by water molecules. Increasing PLA content was not necessarily enhancing the water vapor permeability rate. Dynamic mechanical analysis presented a significant increment in storage modulus (E') for PLA60TPS40 (53.2%) compared to the trivial changes of PLA70TPS30 (10%) and PLA80TPS20 (0.6%). However, significant improvement in impact strength occurred only at PLA40TPS60 (33.13%), and further addition showed minor improvement between 12 and 20%. Overall, it is noted that PLA60TPS40 demonstrated adequate functional properties to be used in food packaging application.

Keywords: dynamic mechanical analysis, impact test, nanocellulose, polymer blend, poly(lactic acid), thermoplastic starch, water barrier properties

*** Corresponding author: Salit Mohd Sapuan,** Laboratory of Biocomposite Technology, Institute of Tropical Forestry and Forest Products (INTROP), Universiti Putra Malaysia, 43400 UPM Serdang, Selangor, Malaysia; Advanced Engineering Materials and Composites Research Centre (AEMC), Department of Mechanical and Manufacturing Engineering, Universiti Putra Malaysia, 43400 UPM Serdang, Selangor, Malaysia, e-mail: sapuan@upm.edu.my
Asmawi Nazrin: Laboratory of Biocomposite Technology, Institute of Tropical Forestry and Forest Products (INTROP), Universiti Putra Malaysia, 43400 UPM Serdang, Selangor, Malaysia
Mohamed Yusoff Mohd Zuhri: Laboratory of Biocomposite Technology, Institute of Tropical Forestry and Forest Products (INTROP), Universiti Putra Malaysia, 43400 UPM Serdang, Selangor, Malaysia; Advanced Engineering Materials and Composites Research Centre (AEMC), Department of Mechanical and Manufacturing Engineering, Universiti Putra Malaysia, 43400 UPM Serdang, Selangor, Malaysia
Intan Syafinaz Mohamed Amin Tawakkal: Department of Process and Food Engineering, Universiti Putra Malaysia, 43400 UPM Serdang, Selangor, Malaysia
Rushdan Ahmad Ilyas: School of Chemical and Energy Engineering, Faculty of Engineering, Universiti Teknologi Malaysia, 81310 Johor Bahru, Johor, Malaysia

1 Introduction

Today, petroleum-based plastics are vastly used in various industries such as packaging, construction, medical, textile, and automotive industries [1–3]. Although the benefits of plastics are wide ranging, massive production and improper waste management have raised environment issues. Production growth is expected to reach 500 million tons by 2050 because of the rise in global population and overall consumption [4]. Single-use plastic (SUP) including plastic bags, microbeads, cutlery, straws, polystyrene such as cups and food containers, and sachet water wrappers are the major contributors to plastic wastes as they are used once and then discarded [5]. Plastics floating in the ocean often mistook as food by marine animals causing serious causalities. Recycling programs are not contributing much in plastic

waste management because of the high recycling cost and difficulties in polymer separation [6,7]. The disposal of plastic wastes through incineration released harmful substances such as dioxins, mercury, furans, and polychlorinated biphenyls into the atmosphere and eventually entered human body system, which were linked with major health issues such as cancer, heart disease, asthma, and respiratory failure [8].

In natural environment, the degradation periods for plastic bags are 10–20 years or 500–1,000 years while plastic bottles are reported up to 70–450 years [9]. This non-biodegradable plastic has unfamiliar compound derived from petroleum making it is inaccessible for microbial organisms to alter or transform (through enzymatic and metabolic action) their chemical structures [10]. The sudden strike of COVID-19 pandemic (a severe acute respiratory syndrome caused by a novel coronavirus – SARS-CoV-2) had severely disrupted the plastic reduction policies because of the consumer concerned over contamination of reusable containers and bags of COVID-19 high transmissibility rate [11]. As the world is concerned over the problems caused by conventional plastics, scientists and researchers are shifting to biodegradable polymers from renewable sources to tackle the accumulation of non-biodegradable plastic wastes.

By far, poly(lactic acid) (PLA) is the most extensively used polymer in the production of biodegradable plastics [12–14]. Unlike other polymers such polyvinylchloride, polyethylene, polypropylene, and epoxy derived from petroleum hydrocarbons, PLA is produced through the fermentation of corn, rice, and sugarcane in the form of lactic acid [15]. However, it is deemed non-economical for such expensive material to be used in the production of SUP applications [16]. The incorporation of starch was used as a means of reducing raw material costs [17] while facilitating biodegradability of PLA [18]. Donate *et al.* [19] incorporated biodegradable and biocompatible materials namely calcium carbonate and beta-tricalcium phosphate into PLA results in faster degradation using proteinase K enzymes compared with neat PLA. Manipulating the additives loading could adjust the degradation rate required in 3D scaffolds to match the growth rate of new bone tissue.

Sugar palm starch (SPS) is yet another promising bioresource used in the manufacturing of bio-based starch films and proven to yield promising features such as biodegradable, colorless, non-toxic, odorless, tasteless, and isotropic [20]. Nevertheless, their brittleness, retrogradation, and low mechanical and water barrier properties have limited their applications [21]. Combination of various plasticizers seemed to reduce starch retrogradation, starch embrittlement, and long-term plasticizer migration and improve water barrier properties [22]. Sanyang *et al.* [23] reported that SPS incorporated with 30% (starch basis) of the combination of glycerol and sorbitol (1:1) improved tensile strength and thermal and water barrier properties compared to glycerol and sorbitol used alone.

The reinforcement of plant-based natural fibers in polymer matrix has become a rising trend because of its outstanding features. Some of their advantages are cheap, low density, biodegradable, renewable, remarkable energy recovery, vibration resistance, and less skin and respiratory irritation [24]. In addition, nanocellulose fibers isolated from sugar palm fibers possess excellent mechanical properties, high surface area (100 $m^2 g^{-1}$), high aspect ratio of 100, light weight, and low density compared to other commercial fibers [25,26]. Even at low content, nanoscale cellulose materials can provide a more effective reinforcement for tensile strength, tensile modulus, and impact strength compared to macroscale natural fiber [27]. In food packaging, using bio-nanocellulose such as sugar palm crystalline nanocellulose (SPCNC) is safer compared to synthetic nanomaterials [28]. Besides, starch and fiber from the same botanical origin seem to have a high affinity of 3D hydrogen bonding networks, thus improving mechanical strength and water barrier properties.

In this research, water barrier, thermal mechanical, impact properties, and crystallinity behavior of SPCNC reinforced TPS/PLA blend bionanocomposites were analyzed with regard to their formulation to identify certain extensions and limitations in developing safer, cheaper, and environmentally friendlier food packaging plastics. To the best of author's knowledge and from the above literature review, no study has been carried out in the past on the performance of SPCNC reinforced thermoplastic sugar palm starch (TPS)/(PLA) blend bionanocomposites. In addition to our previous study [29] that focused on mechanical, physical, and thermal properties, it is crucial to highlight water barrier and thermal mechanical properties, as the exposure to heat and moisture is inevitable in food packaging application causing deterioration in mechanical strength of the material.

2 Materials and methods

2.1 Materials

SPS used in this research was extracted from the core of sugar palm trees located at Kuala Jempol, Negeri Sembilan, Malaysia. PLA resin (NatureWork 2003D), glycerol, and sorbitol were purchased from Mecha Solve Engineering,

Table 1: Physical properties of SPCNC

Properties	Value
Diameter (nm)	9
Density (g/cm^3)	1.05
Degree of crystallinity (%)	85.9
Degree of polymerization	142.86
Moisture content (wt%)	17.90
Molecular weight (g/mol)	23164.7
Pore volume (cm^3/g)	0.226
Surface area (m^2/g)	14.47

Petaling Jaya, Malaysia. Glycerol and sorbitol were used to improve SPS processability. SPCNC was supplied by Laboratory of Biocomposite Technology, Institute of Tropical Forestry and Forest Products (INTROP), Universiti Putra Malaysia, Selangor, Malaysia. Table 1 shows the physical properties of SPCNC.

2.2 SPS extraction and preparation

The mixture of starch and woody fibers was purchased from Hafiz Adha Enterprise at Kampung Kuala Jempol, Negeri Sembilan, Malaysia. The mixture was transferred into a container and left 1 day for the starch to settle at bottom while woody fibers floated at the top. The floating fibers were removed and starch was collected. Strainer cloth was used to filter smaller size of wood fibers mixed with starch. Next, the wet starch was taken out from the container and kept in an open air for a moment. The remaining moisture in the starch was removed by drying in air circulating oven at 120°C for 24 h to obtain starch powder with a mean diameter of 36.308 µm and a particle size distribution ranging from 0.0020 to 1,000 µm. The starch extraction method was adapted from Sahari *et al.* [30].

2.3 Preparation of SPCNC reinforced TPS/PLA blend bionanocomposites sheet

TPS was prepared using solution casting method. First, 0.5 g of SPCNC (0.5%) and 15 g of both glycerol (15%) and sorbitol (15%) were added into beaker filled with 1,000 mL of distilled water. The mixture went through sonication for 15 min to agitate the SPCNC in promoting an even dispersion. Then, the beaker was placed inside the water bath at temperature of 80°C. Gradually, SPS was added into the beaker and stirred continuously for 30–45 min so that the starch gelatinized uniformly. After a semi-fluid consistency was acquired, the gelatinized starch was poured into glass petri dishes and left dried up in the oven at 60°C for 24 h. The dried TPS was crushed into granule-size before being melt blended with PLA using Brabender Plastograph (Model 815651, Brabender GmbH & Co. KG, Duisburg, Germany) at 170°C for 13 min with a rotor speed of 50 rpm. TPS and PLA were mixed in five different ratios as follows: 80:20, 70:30, 60:40, 40:60, and 20:80 (Table 2). The blend bionanocomposites were once again crushed into granule-size before being hot pressed (Technovation, Selangor, Malaysia) at 170°C for 17 min into 150 mm × 150 mm × 3 mm sheet. Figure 1 shows the schematic representation of overall process to prepare PLA/TPS blend bionanocomposites.

2.4 X-ray diffraction (XRD)

The XRD analysis was conducted using 2500 X-ray diffractometer (Rigaku-Tokyo, Japan). The device was managed by 0.02 (θ) s^{-1} scattering speed within 5–60° (2θ) angular range under operating voltage and current of 40 kV and 35 mA, respectively. The crystallinity index (C_i) was measured based on the calculus of crystallinity area (A_c) and amorphous area (A_a) in diffractogram using equation (1).

$$C_i\ (\%) = [A_c/(A_c + A_a)] \times 100. \quad (1)$$

2.5 Moisture content

The moisture content of each sample was determined by the gravimetric method. The sheet samples were stored inside a zip lock plastic bag to prevent moisture absorption from surrounding humidity. Before oven drying, the initial weight (M_1) of the sample was measured. Then, it was left inside an oven at 100°C for 24 h. After 24 h, the final weight was measured (M_2). For each sample, the

Table 2: The composition of PLA/TPS blend bionanocomposites

Samples	PLA (%)	TPS (%)
PLA20TPS80	20	80
PLA40TPS60	40	60
PLA60TPS40	60	40
PLA70TPS30	70	30
PLA80TPS20	80	20
PLA100	100	0

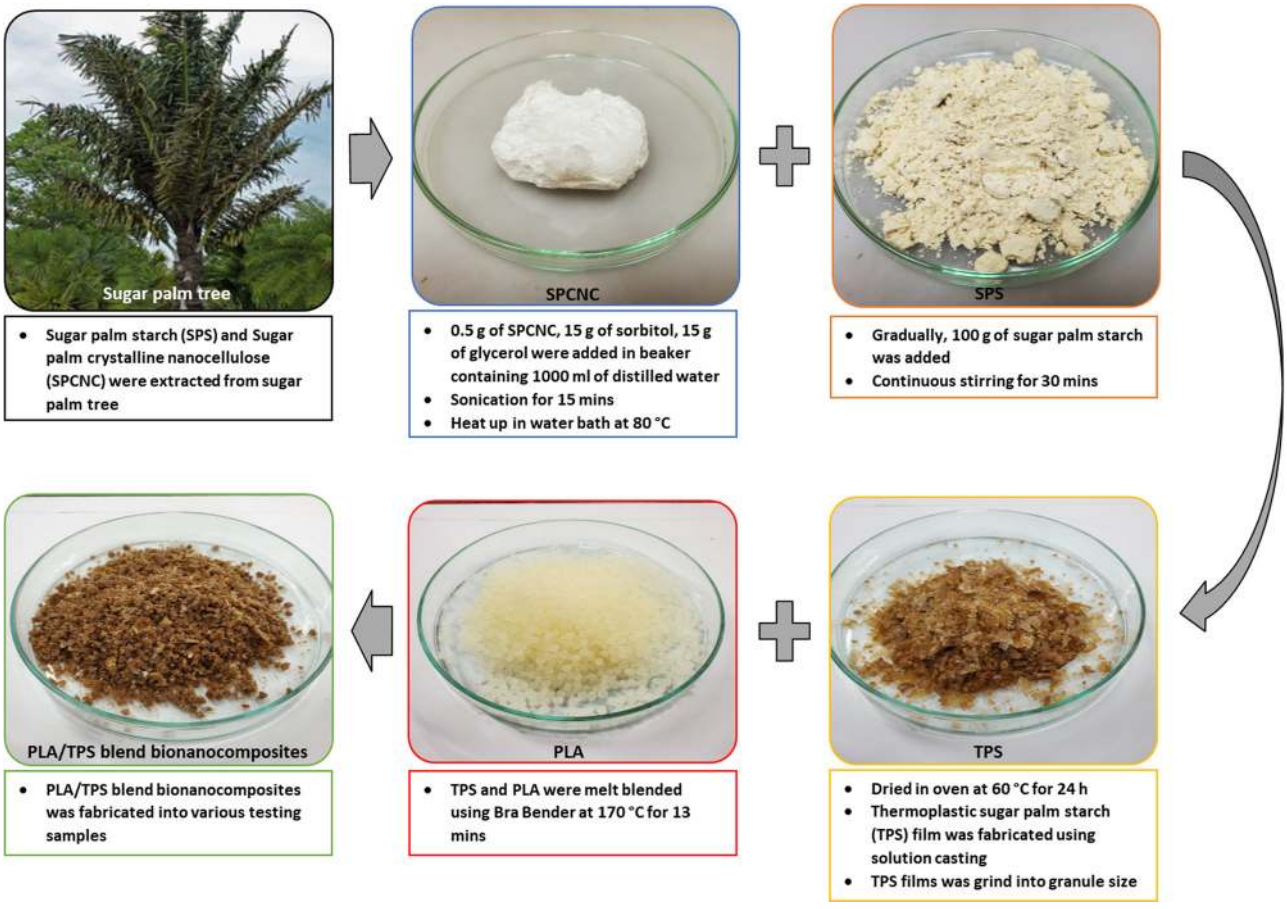

Figure 1: Schematic representation of overall process to prepare PLA/TPS blend bionanocomposites.

experiment was conducted in triplicate. Moisture content of the sample was evaluated as the percentage of the initial weight removed during drying, as shown in equation (2).

$$\text{Moisture content } (\%) = [(M_1 - M_2)/M_1] \times 100. \quad (2)$$

2.6 Water solubility

Solubility test was conducted following the method of Irissin-Mangata *et al.* [31]. Before the test, initial weight (W_1) of each sample (10 mm × 10 mm × 3 mm) was measured. The samples were immersed in water at 25°C under continuous stirring for 24 h. After 24 h, the insoluble remains of the samples were dried at 100°C for another 24 h. Finally, the insoluble dried samples were weighed (W_2). For each sample, the experiment was conducted in triplicate. Water solubility of each blend bionanocomposites was calculated using equation (3).

$$\text{Water solubility } (\%) = [(W_1 - W_2)/W_1] \times 100. \quad (3)$$

2.7 Water vapor permeability (WVP)

WVP was conducted in accordance with ASTM E96-95 [32]. Before the test, the samples were conditioned inside a desiccator under the set of working parameters of 53 ± 1% RH and 23 ± 2°C ambient temperature. The experiment was repeated thrice. Initially, the mouth of the cup (20 mm by diameter) was filled with 10 g of silica gel. Samples were cut into round shapes and mounted on the mouth of cylindrical cups, leaving around 3 mm vacuum to the topmost part. Then, the initial weights of the test cups were measured and recorded before placing them in a steady relative humidity chamber (25°C, 75% RH). The weights of the test cups were measured at regular intervals until the equilibrium state was reached. Finally, the balanced weight of the test cups was measured, noted, and used in the evaluation of WVP as shown in equation (4).

$$\text{Water vapor permeability } (\%) = [(m \times d)/(A \times t \times P)], \quad (4)$$

where the increased weight of the test cup is m (g), the sample thickness is d (mm), the exposed surface area of the sample is A (m^2), the permeation time interval is t (s), and the partial pressure is P (Pa).

2.8 Dynamic mechanical analysis (DMA)

DMA Q800 (New Castle, DE) from TA Instruments was used for the evaluation of the dynamic mechanical thermal behaviors of the composites. DMA was conducted in accordance with ASTM D5053-15 [33]. Samples were cut into rectangular shape with the dimensions of 60 mm (L) × 10 mm (W) × 3 mm (T) and subjected under three-point bending mode in a temperature range between 30 and 150°C at a heating rate of 5°C/min under controlled sinusoidal strain at 1 Hz frequency to determine the temperature dependence of the storage modulus (E'), loss modulus (E''), and loss tangent ($\tan \delta$). The test was performed in three replications.

2.9 Impact test

Impact test measures the strength of a material under dynamic loading. Izod impact test was conducted according to ASTM D256 [34] at a temperature of 23 ± 1°C and relative humidity of 50 ± 5%. Samples were fabricated into V-notched with a depth of 2 mm and an angle of 45° using hot press with dimensions of 64 mm (L) × 13 mm (W) × 3 mm (T). The test was performed in three replications using a digital INSTRON CEAST 9050 (Instron, Norwood, MA, USA) pendulum impact tester. For Izod test, the samples were fixed in vertical position for the pendulum to strike. The impact strength was calculated based on the impact energy required to fracture the sample and cross-section area of the sample as shown in equation (5).

$$\text{Impact strength} = \text{Impact energy (J)/area (mm}^2\text{)}. \quad (5)$$

3 Results and discussion

The results and discussion of the performance of SPCNC reinforced PLA/TPS blend bionanocomposites are presented in the following sections.

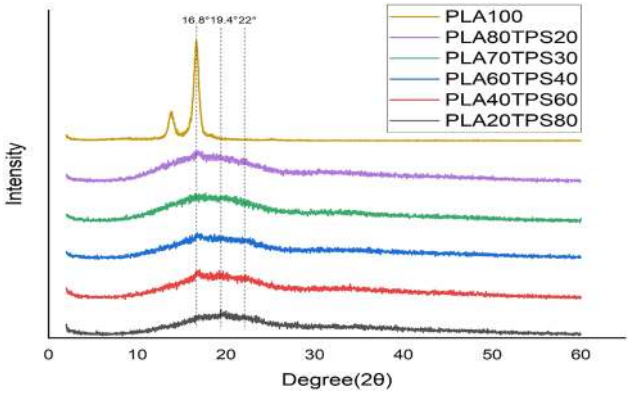

Figure 2: The XRD patterns of neat PLA and PLA/TPS blend bionanocomposites.

3.1 XRD

Figure 2 shows the diffraction patterns of neat PLA and PLA/TPS blend bionanocomposites. Neat PLA exhibited a sharp crystal peak centered at 2θ of 16.8° ascribed to the helical 10^3 chain of PLA [35]. This peak was not visible for the sample with the lowest PLA content (PLA20TPS80), but as PLA contents were increased, the peak gradually appeared indicating its correlation with the content of PLA in the blend. Incorporation of PLA into TPS seemed to form large amorphous scattering background with new minor diffraction peaks at 2θ of 19.4° and 22°. The diffraction peak at 2θ of 19.4° indicated that V_H-type crystal structure was formed by the complexing of plasticizers with amylose [22]. Cotiprayon *et al.* [36] found out that higher content of PLA in PLA/TPS blend composites formed lower and wider diffraction peaks because of the dilution of PLA and migration of glycerol from TPS into PLA matrix. Referring to Figure 2, this diffraction peak disappeared for the samples having more than 50% of PLA content. This implied that all blend bionanocomposite samples were amorphous as PLA obstructed hydrogen bond formation between starch chains by PLA side groups, causing loose packing structure [37]. Diffraction peak at 2θ of 22° corresponded to B-type crystal structure typically for high amylose starches extracted from fruits, stems, and tubers (banana, sago, and potatoes) [38]. The SPCNC reinforcement is also associated with diffraction peak at 2θ of 22° and its lower intensity is linked to the low concentration of SPCNC used in this study [6]. Table 3 shows the crystallinity index of neat PLA and PLA/TPS blend bionanocomposites. Increasing PLA content in the blend seemed to promote the crystallinity

Table 3: Crystallinity index of neat PLA and PLA/TPS blend bionanocomposites

Sample	Crystallinity index, C_i (%)
PLA20TPS80	46.08
PLA40TPS60	53.40
PLA60TPS40	54.35
PLA70TPS30	56.38
PLA80TPS20	59.93
PLA100	71.73

3.2 Moisture content

In Table 4, it can be observed that moisture content decreased as PLA content was increased. The hydrophobic nature of PLA stabilized the moisture content of the blend bionanocomposites. As expected, TPS (which is known for its hydrophilic nature) retained its moisture, which is greatly responsible for the moisture content. In this study, moisture content of the blend bionanocomposites was solely contributed by TPS content. Plasticizers and SPCNC are the factors that manipulated the moisture content of the TPS. Plasticization by combining glycerol and sorbitol is more stable compared to the case when they were used alone. Adhikari *et al.* [39] reported that plasticization using multiple plasticizers might promote strong plasticizer–plasticizer interaction bonds. The presence of SPCNC promoted a stabilization effect in the starch matrix by creating 3D cellulosic network, which hindered the chain mobility and decreased the availability of hydroxyl groups thus resulting in the reduction of moisture absorption [6]. PLA20TPS80, which demonstrated the highest TPS content (80%), undoubtedly consisted of the highest concentration of glycerol, sorbitol, and SPCNC. Li and Huneault [22] reported that additional concentration of glycerol in starch/fiber composites increased their equilibrium moisture but decreased as fiber content was increased. Meanwhile sorbitol did not have any significant increment in equilibrium moisture. However, various authors [21,36,40–42] working on PLA/TPS blend composites found out that glycerol did migrate from TPS into PLA matrix leaving behind sorbitol-rich starch. Higher solubility and lower molecular weight of glycerol (92 g mol^{-1}) compared to sorbitol (182 g mol^{-1}) are more prone to migrate to PLA matrix during melt mixing process [43]. Therefore, primary plasticized TPS using the combination of glycerol and sorbitol was transformed into glycerol-rich PLA/sorbitol-rich starch microstructure [44]. Another important factor that affects the moisture content is the morphology of the blend itself. In previous work [29], because of the absence of compatibilizer to improve the homogeneity of the blend, some blends (above 50% TPS content) displayed slight starch agglomeration on the structure of tensile fracture surface under SEM images. This result shows that the samples, which were formulated using more than half of TPS content in the blend bionanocomposites, provided extra hydroxyl groups for water molecules to interact.

Table 4: Moisture content, solubility, and water vapor permeability of neat PLA and PLA/TPS blend bionanocomposites

Sample	Moisture content (%)	Water solubility (%)	Water vapor permeability, 10^{-11} (g m/m^2 s Pa)
PLA20TPS80	7.41	96.34	1.33
PLA40TPS60	6.72	77.66	1.12
PLA60TPS40	4.97	39.43	1.02
PLA70TPS30	3.46	23.16	1.10
PLA80TPS20	2.51	10.27	1.15
PLA100	0.71	0.57	0.90

3.3 Water solubility

The water solubility of a substance is closely related to biodegradation properties of a material. As shown in Table 4, the solubility of all blend bionanocomposites was influenced by the TPS content. It is observed that PLA20TPS80 has the highest solubility rate (96.34%) and the solubility is decreasing linearly as PLA content increased. A higher PLA content will decrease the amount of hydroxyl groups in the blend, as stated by Muller *et al.* [45]. The solubility of PLA20TPS80 and PLA40TPS60 seemed to be higher than the proportion of TPS in the blend bionanocomposites, suggesting a poor homogeneity. The SEM images reported in ref. [29] verified that both of these samples showed a slight agglomeration of starch granules, which might be the cause of the high solubility. The solubility is directly proportional to the TPS content in the blend bionanocomposites as PLA is insoluble in water. Similar to moisture content, the addition of plasticizers reduced the polymer molecule interaction in return providing greater space in the polymer chains to be penetrated by water molecules, thus maximizing the blend bionanocomposites solubility [46]. The effect of higher moisture content promote starch gelatinization and uniform dispersion in the PLA matrix, thus

increasing surface contact area of the starch phase at the interface [47]. Correspondingly, the contact area of the starch with water on the surface of the sample increased. Both low and high solubility materials benefited various types of application. Low solubility materials are deemed useful in applications, which need protection from moisture and water loss. Meanwhile, high solubility materials can be used as single-use applications such as drug capsulation and biodegradable packaging [48–50]. Lin *et al.* [51] studied the degradation modeling of poly-L-lactide acid (PLLA) as bioresorbable stent or biodegradable stent to serve as a temporary scaffold and found out that the stent kept its mechanical integrity during the first 3 months even though the outer surface of the stent demonstrated degradation.

3.4 Water vapor permeability

As expected, the highest WVP (1.33×10^{-11} g s^{-1} m^{-1} Pa^{-1}) rate is associated with the sample of the highest TPS content (PLA20TPS80). Based on Table 4, it can be observed that the WVP rate decreased as PLA content was increased up to 60% content. At 70% (PLA70TPS30) and 80% (PLA80TPS20) of PLA contents, WVP rates were 1.10×10^{-11} g s^{-1} m^{-1} Pa^{-1} and 1.15×10^{-11} g s^{-1} m^{-1} Pa^{-1}, respectively. This speculated that there might be some passages for water vapor to pass through those samples. The previous work [29] on the SEM analysis showed visible crack-spreading areas within tensile fracture surface of these samples. Ilyas *et al.* [52] fabricated TPS film using SPS reinforced with 0.5% of SPCNC, and the composites improved the WVP significantly by 19.94% compared to neat film (9.58×10^{-10} g s^{-1} m^{-1} Pa^{-1}). However, after blending with PLA, WVP rate elevated even further. Substituting 20% of TPS with PLA was proven to promote WVP rate of the blend bionanocomposites by 98.6%. The reinforcement of SPCNC could not be evaluated in detail because the presence of PLA contributed tremendous impact on WVP. It seems that the main factor that strongly influenced WVP rate is the morphological feature of blend bionanocomposites itself. Unlike moisture content and solubility, dominant PLA content was not necessarily improving the WVP rate. Rather, the compatibility of these two materials is far more crucial in developing homogeneous and uniform distribution of microstructure to prevent particles or gases to pass through it. It seemed that other formulations besides PLA60TPS40 are unable to achieve a decent cross-linking reaction, which increased the chain entanglements of the two polymers.

3.5 DMA

DMA is yet another important method in the characterization of polymer material to determine the miscibility in polymer blends. Sample was exposed to oscillatory deformations under the increment of temperature. It is related to the changes in polymer chains movement, which left some sort of gaps or pores within the polymer chains known as free volume. As temperature rose, tightly packed molecules began to loosen up increasing the free volume.

Figure 3a shows the storage modulus (E') for neat PLA and PLA/TPS blend bionanocomposites as a function of temperature. All curves display a similar trend, where the value of E' dropped sharply within a small temperature range between 50 and 60°C indicating the transition phase of glass into rubber state [53]. In this phase, the molecules expand as they get warm promoting higher molecular chain motions thus changing free volume. Neat PLA or PLA100 has the highest E' value and increasing the incorporation of TPS content into PLA/TPS blend bionanocomposites reduced E'. The sorbitol rich starch within the cross-linked polymers were finely dispersed thanks to their homogeneous ratio, which responsible for PLA60TPS40 (53.3%) significant increase in E' while PLA70TPS30 (10%) and PLA80TPS20 (0.6%) showed trivial changes in E'. As temperature rose, E' dropped indicating the loss in rigidity. The effect of glycerol migration into PLA promoted the chain mobility of the amorphous phases. However, the significant effect of glycerol-rich PLA can only be observed for PLA60TPS40. It is suspected that for PLA70TPS30 and PLA80TPS20, glycerol transfer into PLA matrix was insufficient to enhance the chain mobility which led to minor improvement in E'. The onset temperature where material started to show mechanical failure demonstrated that among all PLA/TPS blend bionanocomposite samples, PLA60TPS40 (63.6°C) had the highest onset temperature comparable to neat PLA (62°C). This shows that the composition of PLA60TPS40 has better compatibility compared to other formulations, thus promoting its thermal stability.

Figure 3b displays the changes in loss modulus (E'') of neat PLA and PLA/TPS blend bionanocomposites. It provides the magnitude of energy released by the sample caused by molecular chain mobility. All blend bionanocomposite samples showed low intensity peak of E'' within the temperature range of 55–70°C. PLA40TPS60, PLA80TPS20, and PLA100 have quite similar peaks approximately at 62°C but with different values of E'' approximately 50, 200, and 550 MPa, respectively. The addition of PLA seemed to increase the intensity peak and temperature only up until PLA60TPS40. At PLA70TPS30,

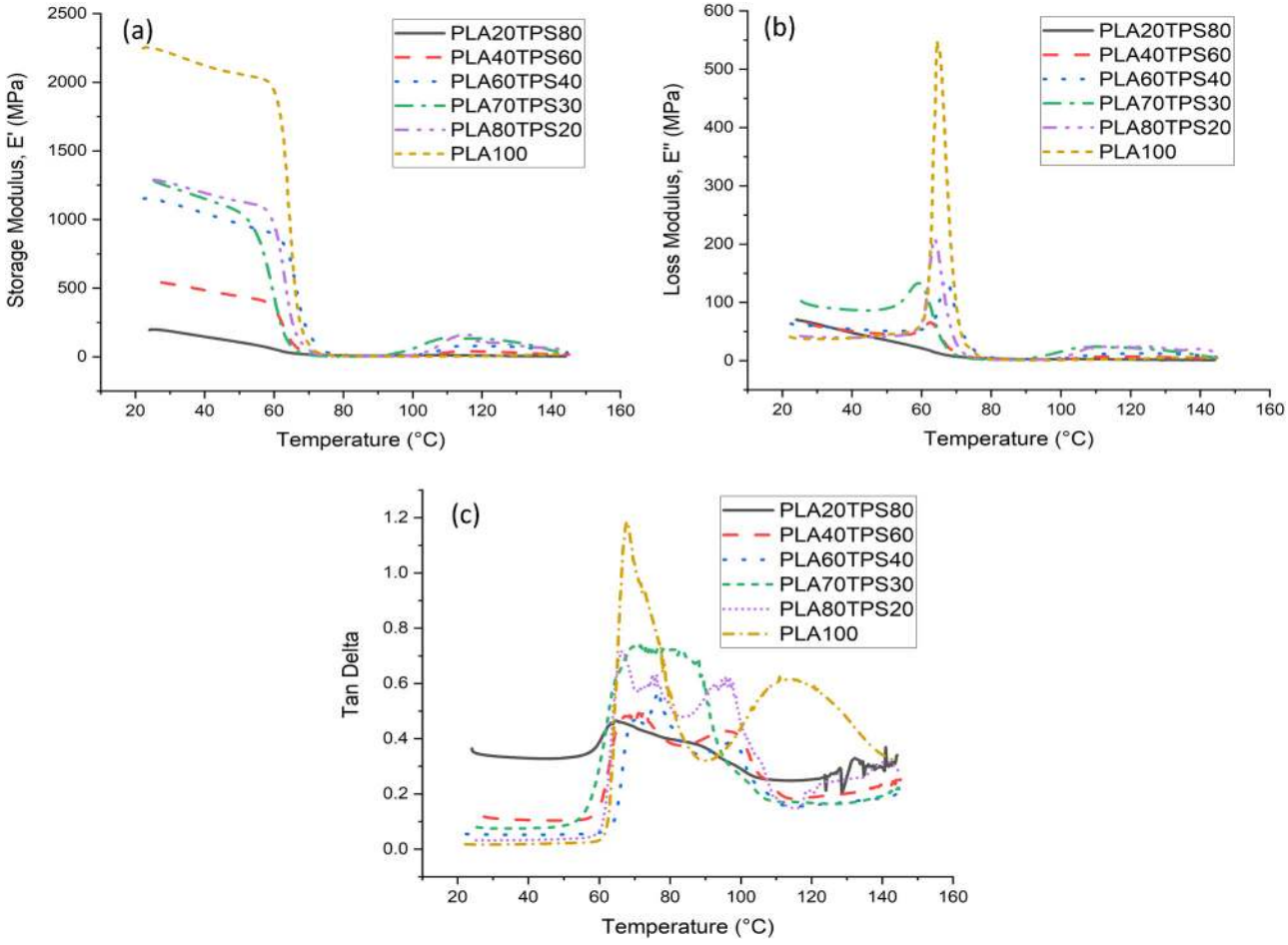

Figure 3: (a) Storage modulus, (b) loss modulus, and (c) tan δ of neat PLA and PLA/TPS blend bionanocomposites.

the peak shifted to lower temperature; meanwhile, there was only a minor increase in PLA80TPS20 temperature, which did not exceed PLA60TPS40. The addition of more rigid and stiffer material reduced the molecular mobility of polymeric chains within the matrix and promoted good frictional resistance, which led to higher loss modulus [54]. Similar increasing trend was achieved by Nurazzi *et al.* [55], where loss modulus of unsaturated polyester hybrid composites increased as sugar palm and glass fibers were increased.

Figure 3c shows the damping factor (tan δ) and glass transition temperature (T_g) for neat PLA and PLA/TPS blend bionanocomposites. Neat PLA has the highest intensity peak, which were followed by PLA/TPS blend bionanocomposites from the lowest to the highest of PLA content. tan δ peaks of all bionanocomposite samples observed to be in the temperature range of 60–80°C. An early increasing trend can be observed within the T_g values of PLA20TPS80, PLA40TPS60, and PLA60TPS40, which were 65, 72, and 76°C respectively. Further addition of PLA decreased the T_g for both PLA70TPS30 and PLA80TPS20, which were 71 and 67°C respectively. With regard to partial miscible polymer blends, the T_g of their components were shifted towards each other gradually. In the case of immiscible polymer blends, the components kept their own T_g. The damping peaks of PLA20TPS80, PLA40TPS60, and PLA60TPS40 were low and within the range to each other. This proved that the fine dispersion of TPS into PLA matrix has the benefit of restricting the segmental motions of polymer during the transition. Akrami *et al.* [56] reported the incorporation 10 phr of synthesized compatibilizer induced esterification to TPS molecules, which results in the reduction of tan δ representing better compatibility of two phases. The damping peaks were shifted to higher value for PLA70TPS30 and PLA80TPS20 indicating poor interfacial adhesion between the polymers. It was also observed in WVP where the poor compatibility of these two samples increased WVP rates even though PLA content was increased. A large area under graph presents the high degree of molecular mobility indicated that the material can absorb and

dissipate energy better. On the contrary, reduction in the intensity of damping peak means that the material acts more elastic and it has better potential to store load rather than dissipating it.

3.6 Impact test

Impact strength is one of the important mechanical data to evaluate material capabilities in various practical applications. It determines the deformation ability of a material when subjected to high deformation rate. Figure 4 shows an increasing trend of impact resistance for neat PLA and PLA/TPS blend bionanocomposites. Initially, it was speculated that the impact resistance of those of blend bionanocomposite samples is higher than the neat PLA itself. Because of the effect of glycerol migration during blending with PLA, higher molecular weight of sorbitol left behind formed strong bond with starch molecular chains, thus restricting its chain mobility and become more rigid leading to the inability to resist deformation. A significant change was observed at PLA40TPS60 (33.13%), while PLA60TPS40 (12.09%) and PLA70TPS80 (12.92%) demonstrated minor changes in impact strength. PLA80TPS20 (19.31%) and PLA100 (20.31%) displayed better improvement in impact strength owing to dominant properties of PLA. The reduction in impact resistance is closely related to the increase in rigidity of a material. Several authors [21,22,57] reported that sorbitol plasticized TPS had better tensile strength but lower elongation at break, while glycerol plasticized TPS had lower tensile but better elongation at break. Sanyang *et al.* [23] studied the effect of different plasticizers (sorbitol and glycerol) and reported that the elongation at break of SPS plasticized by 15% of sorbitol and glycerol were 5.38 and 26.52% respectively. Sahari *et al.* [58] worked on the different concentrations of glycerol (15, 20, 30, and 45%) on SPS and reported that flexural strength and impact resistance increased as glycerol concentration was increased up until 30% of concentration. In addition, SPCNC formed strong interfacial interactions between large surface areas of nanofillers and the starch matrix, which also lead to the increase in the rigidity [59]. Zhang *et al.* [60] worked on PLA/bamboo particle (BP) biocomposites and found out that smaller particle size of BP dispersed uniformly in the PLA matrix and increased cross-linking segment in the PLA matrix, which restricted the molecular chain mobility and consequentially reduced the resistance ability to deform. In theory, the flexibility of TPS was expected to sustain the stresses around the PLA particles, which act to withstand any deformation changes. Unfortunately, in this case, the rigidity of TPS is far greater than the PLA itself, which can be clearly observed in the increment of impact resistance as TPS was substituted by PLA. Because of this occurrence, the increment of impact resistance is associated with sorbitol-rich TPS. In addition, it was observed that high moisture content can be linked to the lower impact strength because moisture or water deteriorates the mechanical properties of starch-based polymer. A high solubility sample proved that the increased surface area contacts of the starch with moisture weaken the sample structure stability leading to the deterioration of sample.

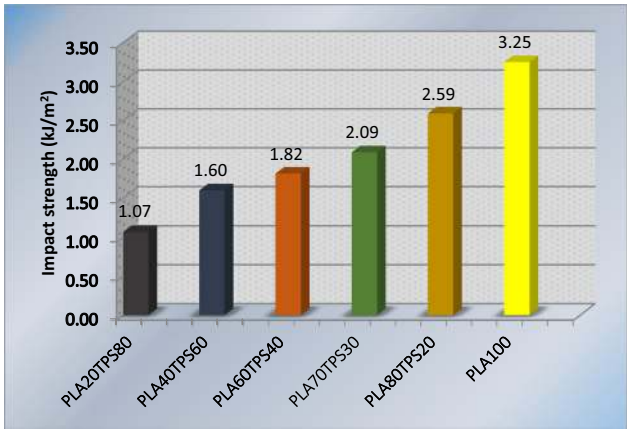

Figure 4: The Izod impact strength of PLA100 and neat PLA/TPS blend bionanocomposites.

4 Conclusion

Generally, the formulation of the PLA/TPS blend bionanocomposites greatly influenced its properties. The ideal ratio to develop food packaging plastic with adequate properties is 60:40 (PLA:TPS). XRD analysis results showed large amorphous scattering background indicating an amorphous structure for all blend bionanocomposite samples because of PLA side groups obstructing hydrogen bond formation between starch chains causing loose packing structure. The superior properties of PLA overwhelm the minor reinforcement of SPCNC in terms of thermomechanical and impact strength properties. The migration of glycerol into PLA matrix reduced the blend flexibility but an ideal ratio and fine dispersion of TPS by sorbitol promoted the blend homogeneity. In case of water barrier properties, improvement in homogeneity promoted the interfacial adhesion between the PLA and TPS lowering water molecules penetration. In addition,

PLA/TPS blend bionanocomposites can also be used in other applications that prioritize biodegradability, adequate water barrier, and mechanical properties such as drug delivery capsule, plastic wrap, and mulching film.

Funding information: The authors wish to thank Universiti Putra Malaysia for the financial support through Geran Putra Berimpak (GPB), UPM/800-3/3/1/GPB/2019/9679800.

Author contributions: All the authors have accepted responsibility for the entire content of this manuscript and approved its submission.

Conflict of interest: The authors state no conflict of interest.

References

[1] Kargarzadeh H, Huang J, Lin N, Ahmad I, Mariano M, Dufresne A, et al. Recent developments in nanocellulose-based biodegradable polymers, thermoplastic polymers, and porous nanocomposites. Prog Polym Sci. 2018;87:197–227. doi: 10.1016/j.progpolymsci.2018.07.008.

[2] Vasile C, Pamfil D, Râpă M, Darie-Niţă RN, Mitelut AC, Popa EE, et al. Study of the soil burial degradation of some PLA/CS biocomposites. Compos Part B Eng. 2018;142:251–62. doi: 10.1016/j.compositesb.2018.01.026.

[3] Geyer R. Production, use, and fate of synthetic polymers. The Boulevard, Langford Lane, Kidlington, Oxford OX5 1GB, UK: Elsevier Inc; 2020. ISBN 9780128178805.

[4] Wang W, Themelis NJ, Sun K, Bourtsalas AC, Huang Q, Zhang Y, et al. Current influence of China's ban on plastic waste imports. Waste Dispos Sustain Energy. 2019;1:67–78. doi: 10.1007/s42768-019-00005-z.

[5] Adam I, Walker TR, Bezerra JC, Clayton A. Policies to reduce single-use plastic marine pollution in West Africa. Mar Policy. 2020;116:103928. doi: 10.1016/j.marpol.2020.103928.

[6] Ilyas RA, Sapuan SM, Ishak MR, Zainudin ES. Development and characterization of sugar palm nanocrystalline cellulose reinforced sugar palm starch bionanocomposites. Carbohydr Polym. 2018;202:186–202. doi: 10.1016/j.carbpol.2018.09.002.

[7] Ge XC, Li XH, Zhu Q, Li L, Meng YZ. Preparation and properties of biodegradable poly(propylene carbonate)/starch composites. Polym Eng Sci. 2004;44:2134–40. doi: 10.1002/pen.20219.

[8] Verma R, Vinoda KS, Papireddy M, Gowda ANS. Toxic pollutants from plastic waste – a review. Procedia Environ Sci. 2016;35:701–8. doi: 10.1016/j.proenv.2016.07.069.

[9] Chamas A, Moon H, Zheng J, Qiu Y, Tabassum T, Jang JH, et al. Degradation rates of plastics in the environment. ACS Sustain Chem Eng. 2020;8:3494–511. doi: 10.1021/acssuschemeng.9b06635.

[10] Shen M, Song B, Zeng G, Zhang Y, Huang W, Wen X, et al. Are biodegradable plastics a promising solution to solve the global plastic pollution? Environ Pollut. 2020;263:114469. doi: 10.1016/j.envpol.2020.114469.

[11] Patrício Silva AL, Prata JC, Walker TR, Campos D, Duarte AC, Soares AMVM, et al. Rethinking and optimising plastic waste management under COVID-19 pandemic: policy solutions based on redesign and reduction of single-use plastics and personal protective equipment. Sci Total Environ. 2020;742:140565. doi: 10.1016/j.scitotenv.2020.140565.

[12] Siakeng R, Jawaid M, Ariffin H, Sapuan SM, Asim M, Saba N. Natural fiber reinforced polylactic acid composites: a review. Polym Compos. 2018;40(2):1–18. doi: 10.1002/pc.24747.

[13] Muller J, González-Martínez C, Chiralt A. Combination of poly (lactic) acid and starch for biodegradable food packaging. Materials (Basel). 2017;10:952. doi: 10.3390/ma10080952.

[14] Castro-Aguirre E, Iñiguez-Franco F, Samsudin H, Fang X, Auras R. Poly(lactic acid) – mass production, processing, industrial applications, and end of life. Adv Drug Deliv Rev. 2016;107:333–66. doi: 10.1016/j.addr.2016.03.010.

[15] Sanyang ML, Sapuan SM, Jawaid M, Ishak MR, Sahari J. Development and characterization of sugar palm starch and poly(lactic acid) bilayer films. Carbohydr Polym. 2016;146:36–45. doi: 10.1016/j.carbpol.2016.03.051.

[16] Nofar M, Sacligil D, Carreau PJ, Kamal MR, Heuzey MC. Poly (lactic acid) blends: processing, properties and applications. Int J Biol Macromol. 2019;125:307–60. doi: 10.1016/j.ijbiomac.2018.12.002.

[17] Zhang S, Feng X, Zhu S, Huan Q, Han K, Ma Y, et al. Novel toughening mechanism for polylactic acid (PLA)/starch blends with layer-like microstructure via pressure-induced flow (PIF) processing. Mater Lett. 2013;98:238–41. doi: 10.1016/j.matlet.2012.12.019.

[18] Nazrin A, Sapuan SM, Zuhri MYM, Ilyas RA, Syafiq R, Sherwani SFK. Nanocellulose reinforced thermoplastic starch (TPS), polylactic acid (PLA), and polybutylene succinate (PBS) for food packaging applications. Front Chem. 2020;8:1–12. doi: 10.3389/fchem.2020.00213.

[19] Donate R, Monzón M, Alemán-Domínguez ME, Ortega Z. Enzymatic degradation study of PLA-based composite scaffolds. Rev Adv Mater Sci. 2020;59:170–5. doi: 10.1515/rams-2020-0005.

[20] Ilyas RA, Sapuan SM, Ibrahim R, Abral H, Ishak MR, Zainudin ES, et al. Effect of sugar palm nanofibrillated cellulose concentrations on morphological, mechanical and physical properties of biodegradable films based on agro-waste sugar palm (Arenga pinnata (Wurmb.) Merr) starch. J Mater Res Technol. 2019;8:4819–30. doi: 10.1016/j.jmrt.2019.08.028.

[21] Mohammadi Nafchi A, Moradpour M, Saeidi M, Alias AK. Thermoplastic starches: properties, challenges, and prospects. Starch – Stärke. 2013;65:61–72. doi: 10.1002/star.201200201.

[22] Li H, Huneault MA. Comparison of sorbitol and glycerol as plasticizers for thermoplastic starch in TPS/PLA blends. J Appl Polym Sci. 2011;119:2439–48. doi: 10.1002/app.32956.

[23] Sanyang ML, Sapuan SM, Jawaid M, Ishak MR, Sahari J. Effect of plasticizer type and concentration on tensile, thermal and barrier properties of biodegradable films based on sugar palm (Arenga pinnata) starch. Polymers (Basel). 2015;7:1106–24. doi: 10.3390/polym7061106.

[24] Alhijazi M, Zeeshan Q, Qin Z, Safaei B, Asmael M. Finite element analysis of natural fibers composites: a review.

Nanotechnol Rev. 2020;9:853–75. doi: 10.1515/ntrev-2020-0069.
[25] Ilyas Rushdana A, Sapuan Salit M, Lamin Sanyang M, Ridzwan Ishak M. Nanocrystalline cellulose as reinforcement for polymeric matrix nanocomposites and its potential applications: a review. Curr Anal Chem. 2017;13:203–25. doi: 10.2174/1573411013666171003155624.
[26] Ilyas RA, Sapuan SM, Ishak MR. Isolation and characterization of nanocrystalline cellulose from sugar palm fibres (Arenga Pinnata). Carbohydr Polym. 2018;181:1038–51. doi: 10.1016/j.carbpol.2017.11.045.
[27] Yu T, Soomro SA, Huang F, Wei W, Wang B, Zhou Z, et al. Naturally or artificially constructed nanocellulose architectures for epoxy composites: a review. Nanotechnol Rev. 2020;9:1643–59. doi: 10.1515/ntrev-2020-0116.
[28] Syafiq RMO, Sapuan SM, Zuhri MRM. Effect of cinnamon essential oil on morphological, flammability and thermal properties of nanocellulose fibre-reinforced starch biopolymer composites. Nanotechnol Rev. 2020;9:1147–59. doi: 10.1515/ntrev-2020-0087.
[29] Nazrin A, Sapuan SM, Zuhri MYM. Mechanical, physical and thermal properties of sugar palm nanocellulose reinforced thermoplastic starch (TPS)/poly(lactic acid) (PLA) blend bionanocomposites. Polymers (Basel). 2020;12:2216. doi: 10.3390/polym12102216.
[30] Sahari J, Sapuan SM, Zainudin ES, Maleque MA. Thermo-mechanical behaviors of thermoplastic starch derived from sugar palm tree (Arenga pinnata). Carbohydr Polym. 2013;92:1711–6. doi: 10.1016/j.carbpol.2012.11.031.
[31] Irissin-Mangata J, Bauduin G, Boutevin B, Gontard N. New plasticizers for wheat gluten films. Eur Polym J. 2001;37:1533–41. doi: 10.1016/S0014-3057(01)00039-8.
[32] ASTM E96/E96M-16. Standard test methods for water vapor transmission of materials. West Conshohocken, PA: ASTM International; 2016. www.astm.org
[33] ASTM D5023-15. Standard test method for plastics: dynamic mechanical properties: in flexure (three-point bending). West Conshohocken, PA: ASTM International; 2015. www.astm.org
[34] ASTM D256-10(2018). Standard test methods for determining the Izod pendulum impact resistance of plastics. West Conshohocken, PA: ASTM International; 2018. www.astm.org
[35] Muller J, González-Martínez C, Chiralt A. Poly(lactic) acid (PLA) and starch bilayer films, containing cinnamaldehyde, obtained by compression moulding. Eur Polym J. 2017;95:56–70. doi: 10.1016/j.eurpolymj.2017.07.019.
[36] Chotiprayon P, Chaisawad B, Yoksan R. Thermoplastic cassava starch/poly(lactic acid) blend reinforced with coir fibres. Int J Biol Macromol. 2020;156:960–8. doi: 10.1016/j.ijbiomac.2020.04.121.
[37] Noivoil N, Yoksan R. Oligo(lactic acid)-grafted starch: a compatibilizer for poly(lactic acid)/thermoplastic starch blend. Int J Biol Macromol. 2020;160:506–17. doi: 10.1016/j.ijbiomac.2020.05.178.
[38] Dome K, Podgorbunskikh E, Bychkov A, Lomovsky O. Changes in the crystallinity degree of starch having different types of crystal structure after mechanical pretreatment. Polymers (Basel). 2020;12:1–12. doi: 10.3390/polym12030641.
[39] Adhikari B, Chaudhary DS, Clerfeuille E. Effect of plasticizers on the moisture migration behavior of low-amylose starch films during drying. Dry Technol. 2010;28:468–80. doi: 10.1080/07373931003613593.
[40] Petchwattana N, Sanetuntikul J, Narupai B. Plasticization of biodegradable poly(lactic acid) by different triglyceride molecular sizes: a comparative study with glycerol. J Polym Environ. 2018;26:1160–8. doi: 10.1007/s10924-017-1012-7.
[41] Wu D, Hakkarainen M. Recycling PLA to multifunctional oligomeric compatibilizers for PLA/starch composites. Eur Polym J. 2015;64:126–37. doi: 10.1016/j.eurpolymj.2015.01.004.
[42] Teixeira EDM, Curvelo AAS, Corrêa AC, Marconcini JM, Glenn GM, Mattoso LHC. Properties of thermoplastic starch from cassava bagasse and cassava starch and their blends with poly (lactic acid). Ind Crops Prod. 2012;37:61–8. doi: 10.1016/j.indcrop.2011.11.036.
[43] Teixeira EdeM, Pasquini D, Curvelo AAS, Corradini E, Belgacem MN, et al. Cassava bagasse cellulose nanofibrils reinforced thermoplastic cassava starch. Carbohydr Polym. 2009;78:422–31. doi: 10.1016/j.carbpol.2009.04.034.
[44] Esmaeili M, Pircheraghi G, Bagheri R, Altstädt V. Poly(lactic acid)/coplasticized thermoplastic starch blend: effect of plasticizer migration on rheological and mechanical properties. Polym Adv Technol. 2019;30:839–51. doi: 10.1002/pat.4517.
[45] Müller CMO, Pires ATN, Yamashita F. Characterization of thermoplastic starch/poly(lactic acid) blends obtained by extrusion and thermopressing. J Braz Chem Soc. 2012;23:426–34. doi: 10.1590/s0103-50532012000300008.
[46] Ibrahim MIJ, Sapuan SM, Zainudin ES, Zuhri MYM. Physical, thermal, morphological, and tensile properties of cornstarch-based films as affected by different plasticizers. Int J Food Prop. 2019;22:925–41. doi: 10.1080/10942912.2019.1618324.
[47] Ke T, Sun X. Effects of moisture content and heat treatment on the physical properties of starch and poly(lactic acid) blends. J Appl Polym Sci. 2001;81:3069–82. doi: 10.1002/app.1758.
[48] Preechawong D, Peesan M, Supaphol P, Rujiravanit R. Preparation and characterization of starch/poly(l-lactic acid) hybrid foams. Carbohydr Polym. 2005;59:329–37. doi: 10.1016/j.carbpol.2004.10.003.
[49] Cai J, Liu M, Wang L, Yao K, Li S, Xiong H. Isothermal crystallization kinetics of thermoplastic starch/poly(lactic acid). composites Carbohydr Polym. 2011;86:941–7. doi: 10.1016/j.carbpol.2011.05.044.
[50] Lv S, Zhang Y, Gu J, Tan H. Physicochemical evolutions of starch/poly (lactic acid) composite biodegraded in real soil. J Environ Manage. 2018;228:223–31. doi: 10.1016/j.jenvman.2018.09.033.
[51] Lin S, Dong P, Zhou C, Dallan LAP, Zimin VN, Pereira GTR, et al. Degradation modeling of poly-L-lactide acid (PLLA) bioresorbable vascular scaffold within a coronary artery. Nanotechnol Rev. 2020;9:1217–26. doi: 10.1515/ntrev-2020-0093.
[52] Ilyas RA, Sapuan SM, Ishak MR, Zainudin ES. Sugar palm nanocrystalline cellulose reinforced sugar palm starch composite: degradation and water-barrier properties. IOP Conf Ser Mater Sci Eng. 2018;368:012006. doi: 10.1088/1757-899X/368/1/012006.
[53] Raghu N, Kale A, Raj A, Aggarwal P, Chauhan S. Mechanical and thermal properties of wood fibers reinforced poly(lactic acid)/thermoplasticized starch composites. J Appl Polym Sci. 2018;135:1–10. doi: 10.1002/app.46118.
[54] Senthilkumar K, Saba N, Chandrasekar M, Jawaid M, Rajini N, Siengchin S, et al. Compressive, dynamic and thermo-

mechanical properties of cellulosic pineapple leaf fibre/polyester composites: influence of alkali treatment on adhesion. Int J Adhes Adhes. 2021;106:102823. doi: 10.1016/j.ijadhadh.2021.102823.

[55] Nurazzi NM, Khalina A, Sapuan SM, Ilyas RA, Rafiqah SA, Hanafee ZM. Thermal properties of treated sugar palm yarn/glass fiber reinforced unsaturated polyester hybrid composites. J Mater Res Technol. 2020;9:1606–18. doi: 10.1016/j.jmrt.2019.11.086.

[56] Akrami M, Ghasemi I, Azizi H, Karrabi M, Seyedabadi M. A new approach in compatibilization of the poly(lactic acid)/thermoplastic starch (PLA/TPS) blends. Carbohydr Polym. 2016;144:254–62. doi: 10.1016/j.carbpol.2016.02.035.

[57] Soares FC, Yamashita F, Müller CMO, Pires ATN. Thermoplastic starch/poly(lactic acid) sheets coated with cross-linked chitosan. Polym Test. 2013;32:94–8. doi: 10.1016/j.polymertesting.2012.09.005.

[58] Sahari J, Sapuan SM, Zainudin ES, Maleque MA. Flexural and impact properties of biopolymer derived from sugar palm tree. Adv Mater Res. 2013;701:225–8. doi: 10.4028/www.scientific.net/AMR.701.225.

[59] Thompson L, Azadmanjiri J, Nikzad M, Sbarski I, Wang J, Yu A. Cellulose nanocrystals: production, functionalization and advanced applications. Rev Adv Mater Sci. 2019;58:1–16. doi: 10.1515/rams-2019-0001.

[60] Zhang S, Liang Y, Qian X, Hui D, Sheng K. Pyrolysis kinetics and mechanical properties of poly(lactic acid)/bamboo particle biocomposites: effect of particle size distribution. Nanotechnol Rev. 2020;9:524–33. doi: 10.1515/ntrev-2020-0037.